Journal of ELECTRICAL ENGINEERING, VOL. 52, NO. 7-8, 2001, 187–192

CAPABILITIES AND LIMITATIONS OF COHERENT OPTICAL FREQUENCY–DOMAIN REFLECTOMETRY

Jozef Jasenek *

The detail theoretical analysis of the Coherent-optical Frequency-domain Reflectometry as a method for the recovery of the back-scattered signal and Fresnel reflections in the SM optical fiber is given. The main performance limitations of the method are discussed and the basic conclusions applicable in the design and use of the C-OFDR reflectometer are given.

K e y w o r d s: optical reflectometry, OTDR, optical waveguides, coherent optics

1 INTRODUCTION

Optical time-domain reflectometry (OTDR), originally developed by Barnoski and Jensen in 1976 [1], is now a well-established tool for non-destructive characterization of optical networks and components. In general an ideal reflectometry system would have a spatial resolution high enough to locate closely separated sites of reflection within the network under test. In addition the sensitivity would be high enough to measure Raileygh back scattering through fiber network. Time domain techniques using OTDR are generally used for a measurement range up to hundreds of kilometers and the resolution of a few centimeters can be achieved. The typical dynamical range is about 40-50 dB, while the sensitivity is limited to -60 dB. OTDR is also widely used in sensor applications [2].

In OTDR techniques where the system is probed by narrow pulses of optical radiation, the spatial resolution can be improved as the pulses are shortened and the measurement band-width is broadened. However, it results in an increase of the noise level and consequently in a decrease of the dynamical range (well-known trade-off between dynamical range and space resolution). To solve this problem other approaches to optical reflectometry in time domain were and are permanently being search for. To this time we can speak about the correlation OTDR based on the use of pseudorandom probe signal [3] or on the use of complementary Golay code probe signal [4], the photon-counting OTDR [5], and the low correlation OTDR [6]. Each of these OTDR modifications is characteristic by some advantages and drawbacks that determine the field of its utilization. For instance the low-correlation OTDR, which is characteristic with very high sensitivity (under -150 dB) and space resolution (tens of μm), is predominantly used for the characterization of miniature integrated optical waveguides.

Another approach is the coherent optical frequency domain reflectometry (C-OFDR), often called also frequency-modulated continuous-wave reflectometry (FMCW) in which the probe signal is a continuous frequency modulated optical wave [7]. In contrast to OTDR the C-OFDR systems which use more energetic continuous wave probing are characteristic by a dynamical range that does not depend on the space resolution. This significant feature gives the C-OFDR the potential to achieve a high spatial resolution without the loss of dynamical range. Combination of this technique with an coherent detection scheme gains the additional advantage - high sensitivity. Sensitivities down to -100 dB and space resolution in millimeter range can be achieved. Comparing the performance parameters of classical OTDR and the low correlation OTDR one can state that C-OFDR fulfils the gap between the two mentioned extremes. It is determined for characterization of optical lines of medium length and with higher space resolution (LAN).

A crucial element in the C-OFDR is the optical source, which strongly influences the achievable spatial resolution and measurement range. High spatial resolution requires the highly coherent source having a broad, phase-continuous and simultaneously linear tuning range. However, real sources depart from perfect coherence and produce phase noise that limits the system performance. First - it limits the distance over which the discrete reflections can be measured and second - it decreases the dynamical range between the reflected signal of interest and the level of phase noise. For a long time the lack of suitable sources was the main objection for a broader utilization of C-OFDR in practice. The progress in technology of semiconductor laser diodes and fiber lasers during a few recent years brought new promises for the use of this technique. Special three electrode laser diodes made possible to achieve a space resolution of 400 μm and to measure the back scattered signals on fibers 400 m long [8]. The use of laser diodes with external fiber resonators allows to enhance the coherence length and to increase the measurement range to several hundred meters [9]. C-

* Slovak University of Technology, Faculty of Electrical Engineering and Information Technology, Department of Electromagnetic Theory, Ilkovičova 3, 812 19 Bratislava, Slovakia

ISSN 1335-3632

OFDR instrument based on the use of a tunable fiber laser with a very narrow line-width (10 kHz) tuned mechanically by a piezo-electric transducer makes possible to measure the reflectivity on the level -110 dB with 80 dB dynamical range. The narrow line width of the source allows long-range measurement, at 150 m, with a spatial resolution of 16 cm [10].

In this paper a detail theoretical analysis of the C-OFDR for the recovery of distributed back scattered light and discrete Fresnel reflections along the optical fiber is given. The important limitation factors of the method such as the phase noise, the influence of polarization fluctuation, mode hopping and the distortion by frequency modulation non-linearity are briefly discussed and the possible solutions are outlined.

2 THEORETICAL BACKGROUND OF C–OFDR

The basic idea of the C-OFDR can be explained using the simplified block diagram of the C-OFDR reflectometer as illustrated in the Fig. 1.

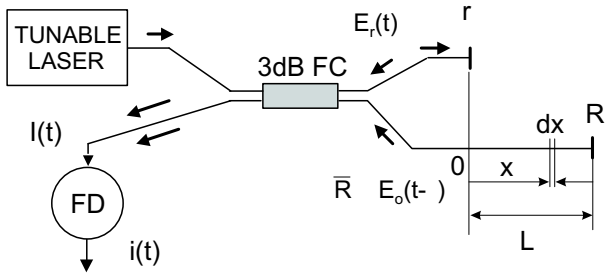

Fig. 1. Simplified block diagram of the C-OFDR based reflectometer, FC - fiber coupler, FD - photodetector

The CW optical radiation generated by a highly coherent laser diode is slowly and linearly swept around the central frequency ω_0 and coupled into the Michelson fiber interferometer. The reference arm of the interferometer is terminated by a mirror and the test arm is coupled to the fiber under test. The time delay between the signals from the reflector in the reference arm and the backscattered signal from an arbitrary element $\mathrm{d}x$ at position x in the test arm is $\tau = 2x/v_g$, where v_g is the group velocity in the fiber core. For coherent detection, both signals are mixed at the detector. During the time delay τ the linearly swept optical frequency changes by $\Omega\tau(\mathrm{d}\omega/\mathrm{d}t)$. This subtraction frequency component can be observed in the detector signal using the optical spectrum analyzer. Its frequency Ω determines the position x on the fiber. The amplitude of this component is proportional to the local back scattering coefficient and optical power. The local optical power is proportional to the factor $e^{-2\alpha x}$ that describes the forward and backward signal attenuation on the distance x. Performing the Fourier transform of the detector signal in a low frequency spectrum analyzer one can simultaneously observe the back scattered waves from all points along the fiber under test. They correspond directly to the frequency axes Ω of the analyzer.

For a more detail description of the method let us consider a light wave of the amplitude E_0 coupled at position $x = 0$ into the single mode test fiber of length L, see Fig. 1. In complex representation we can describe the electric intensity wave amplitude by $E(x)e^{-i\beta x}$, where β is the propagation constant and $E(x) = a^{1/2}E_0$ is the real amplitude with an attenuation function $a(x)$ defined by

$$a(x) = e^{-\int_0^x \alpha(\xi)d\xi}. \tag{1}$$

This function is to be determined from the measurement data. Superposition of all back- scattered signals, coming from particular elementary fiber sections $\mathrm{d}x$ to the input fiber end, is given by the integral

$$E_0(0,\beta) = E_0 \int_0^L \sigma(x)a(x)e^{-i2\beta x}dx \tag{2}$$

As it was mentioned above, the optical frequency ω is linearly swept and consequently also the propagation constant $\beta(t) = \omega(t)/v_g = \beta_0 + \gamma t$ changes linearly in some interval $\Delta\beta$. γ is the sweep rate, $\gamma = (1/v_g)d\omega\mathrm{d}t$ The principle of C-OFDR consists in the measurement of the function $E(0,t)$ as a function of t and in subsequent performing of Fourier transform to convert the data into the space domain.

The reference wave $E_r(0,t) = rE_0a(x_r)e^{-i2\beta(t)x_r}$, produced by a discrete reflection of forward wave in reference arm from the Fresnel reflector at position x_r with the reflection coefficient r, interferes at the detector with the total back scattered wave from the measurement arm, given by relation (2). The photodetector current $i(t)$ is proportional to the intensity of interfering waves $I(t) = |E_q + E_r|^2 = |E_0|^2 + |E_r|^2 + E_0^*E_r + E_0E_r^*$. The DC part of the photo current, given by the first two terms, does not depend on β, while the last two terms representing the AC current part depend on β. It is suitable to define the complex normalized back scattered signal $e(\beta) = E_0(0,\beta)/E_r(0,\beta)$. Real part of $e(\beta)$ can be directly measured. Combining the expressions for $E_0(0,\beta)$ and $E_r(0,\beta)$ we can write

$$e(t) = \frac{1}{2\pi}\int_0^L E(x)e^{-i2(x-x_r)\gamma t}dx \tag{3}$$

$$E(x) = 2\pi\frac{\sigma(x)a(x)}{ra(x_r)}e^{-i2\beta_0(x-x_r)} \tag{4}$$

Looking at relation (3) one can see that the back scattered signal from point x contributes to the total AC normalized signal at the photo detector by the signal with amplitude $E(x)\mathrm{d}x$ and frequency $\Omega = 2\gamma|x - x_r|$, which is

the beating frequency of both reference and measurement arm signals coming from points x and x_r respectively.

Frequency Ω depends besides x also on the choice of reference point x_r. If we take $x_r = 0$, then the highest frequency $\Omega_m = 2\gamma L$ and each position on the fiber is associated unambiguously with the frequency $\Omega/\Omega_m = 2\gamma x/L$, which we can directly observe on the screen of a spectrum analyzer. By a suitable choice of γ and L one can find the $\Omega/2\pi$ in the range of tens or hundreds of Hz.

Integral (3) can be looked at as the inverse Fourier transform of spectral function $E(\Omega) = E(2\gamma|x - x_r|) = E(x)$. But the function $E(x)$ has to be recovered. To do this one has to perform the direct Fourier transform of measured function $e(t)$ as follows

$$E(\Omega) = \int_{-\infty}^{\infty} e(t)e^{-i\Omega t}\mathrm{d}t \tag{5}$$

However, the frequency sweeping $\Delta\omega = \gamma\Delta t$ is limited to a rather short period Δt and the integral (5) can not be calculated on the whole time axis, the integration therefore must be truncated what is equivalent to the multiplication of $e(t)$ by a rectangular impulse shape function of unit height and Δt width before performing the integration (5). As a consequence, the recovered function $E_R(\Omega)$ will be given by the convolution of both spectra

$$E_R(\Omega) = E(\Omega) \otimes R(\Omega) \tag{6}$$

or in space coordinates

$$E_R(x) = E(x) \otimes R(x) \tag{7}$$

where $R(\Omega)$ or $R(x)$ are the spectral function of the impulse function in frequency domain or space domain respectively. Because $R(\Omega)$ and $R(x)$ are sinc functions, we can approximate the space resolution of the method by relations

$$\Delta\Omega = \frac{2\pi}{\Delta t} \qquad \text{and} \qquad \Delta x = \frac{2\pi}{\Delta\beta}. \tag{8}$$

For this reason it is not possible to recover two reflections on the fiber that are mutually separated by a distance smaller than Δx given by (8). With contemporary available optical sources and their tuning possibilities Δx can be made less than 1 mm.

In practice the approximate function $E_R(x)$ is reconstructed by sampling the back-scattered signal in a series of M points in time interval Δt and integral (5) is evaluated numerically in the low frequency spectrum analyzer. However, because the complex scattering factor $\sigma(x)$ in (4) is of statistical nature (as for the magnitude and phase) the reconstructed function $E_R(x)$ is very ragged. This problem can be solved by repeating the measurement process m - times and using the average data in the numerical calculation. It can be shown that applying this procedure the resulting averaged function $E_{Rav}(x)$ will then have the relative standard deviation proportional to $0.5\sqrt{(}m)$. Using (4) for the recovered function $E_{Rav}(x)$ gives

$$E_{Rav}(x) = \frac{\sigma_{2\beta_0}(x)a(x)}{ra(x_r)} \tag{9}$$

where $\sigma_{2\beta 0}$ is essentially the Fourier coefficient of $\sigma(x)$ at spatial frequency $2\beta_0$, evaluated over the uncertainty interval Δx centered at x. Using (9) and (1) the local attenuation coefficient $\alpha(x)$ can now be determined in a straightforward way as

$$\alpha(x) = \mp\frac{\mathrm{d}}{\mathrm{d}x}\ln|E_{Rav}(x)| \tag{10}$$

where the sign "-" holds for $x_r = 0$ and + for $x_r = L$.

3 LIMITATION BY THE OPTICAL SOURCE COHERENCE LENGTH AND PHASE NOISE

In the previous section we have concentrated on the recovery of the back scattered signal from the measured data by C-OFDR method assuming that the optical source is nearly monochromatic. But real sources generate significant amount of phase noise which is manifested by a finite source spectral line width $\Delta\nu_0$. As we shall show the influence of the noise is detrimental in C-OFDR measurement. *It decreases the space resolution and limits the length of the fiber on which reliable measurements can be done. Furthermore it also shortens the section of the fiber on which the back-scattered signal and strong Fresnel reflections can be simultaneously measured.*

To analyze this topic in detail let us consider only the two signals generated by the Fresnel reflections at the ends of reference and measurement arms of the interferometer with the reflections coefficients r and R respectively, see Fig. 1. For our purposes here we do not take into account the back-scattered signal (which is much more smaller). It is evident that the time delay τ_0 between the two signals is $\tau_0 = 2x_0/v_g$, where v_g is the group velocity in fiber core. As we have already shown the goal of the C-OFDR measurement is to acquire the picture of the spectral power density of the detected signal. We do it here by calculating the auto-correlation function of the detector photocurrent $i(t)$ and by subsequent performing its Fourier transform. For this purpose, similarly as before, we can write for the photocurrent $i(t)$ the following relation

$$i(t) = |E(t) + \sqrt{R}E(t - \tau_0)|^2, \tag{11}$$

where we assume the use of a 3 dB fiber coupler and $r = 1$. The unimportant constant factor is omitted here. The electric field intensity $E(t)$ is now given by

$$E(t) = E_0 e^{j(\omega_0 + \pi\gamma t)t + \Phi_t}, \tag{12}$$

where Φ_t is the randomly fluctuating optical phase of the optical source at time t. Combining (11) and (12) gives the final relation for the photocurrent

$$\begin{aligned} i(t) =& E_0^2[1 + R + 2\sqrt{R}\cos(\omega_b t + \omega_0\tau_0 - \\ & - \frac{1}{2}\omega_0\tau_0 + \Phi_t - \Phi_{t-\tau_0})]. \end{aligned} \tag{13}$$

The photocurrent beat frequency is now defined by $\omega_b = 2\pi\gamma\tau_0$. According to the definition the normalized autocorrelation function $F_i(T)$ of the photocurrent $i(t)$ is given by

$$\begin{aligned} F_i(T) =& \left(\frac{1}{E_0^2}\right)\langle i(t)i(t+T)\rangle = (1+R)^2 + \\ & + 2R\cos\omega_b T\langle\cos[(\Phi_{t+T} - \Phi_t) - (\Phi_{t-\tau_0+T} - \Phi_{t-\tau_0})]\rangle \\ & - 2R\sin\omega_b T\langle\sin[(\Phi_{t+T} - \Phi_t) - (\Phi_{t-\tau_0+T} - \Phi_{t-\tau_0})]\rangle. \end{aligned} \tag{14}$$

Here the $\langle\rangle$ represents time averaging. If the change of Φ_t is a random variable with zero mean value, the phase changes over non-overlapping time period are statistically independent. For that case and for $|T| \le \tau_0$, (14) can be written in the form

$$\begin{aligned} F_{i1}(T) =& (1+R)^2 + 2R\cos\omega_b T\langle\cos(\Phi_{t+T} - \Phi_t)\rangle \\ & \langle\cos(\Phi_{t-\tau_0+T} - \Phi_{t-\tau_0})\rangle = \\ =& (1+R)^2 + 2R\cos\omega_b T e^{-\frac{2|T|}{\tau_c}}. \end{aligned} \tag{15}$$

For $|T| \ge \tau_0$ it is

$$F_{i2}(T) = (1+R)^2 + 2R\cos\omega_b T e^{-\frac{2\tau_0}{\tau_c}}. \tag{16}$$

In these calculations the relation $\langle\cos\Phi_\tau\rangle = e^{-1/2\langle\Delta\Phi_\tau^2\rangle}$, $\langle\sin\Delta\Phi_\tau\rangle = 0$, $\langle\Delta\Phi_\tau^2\rangle = \langle(\Phi_t au - \Phi)_{t-\tau}^2\rangle = 2\pi|\tau|\Delta v_0$, $\Delta v_0 = 1/(\pi\tau_c)$, where Δv_0 and τ_c are the optical source spectral line width and its coherence time respectively. Tacitly we have assumed that the optical source is a Lorentzian one.

Generally, the Fourier transform of the autocorrelation function $F_i(t)$ is defined by the integral

$$\begin{aligned} S_i =& \int_{-\infty}^{\infty} F_i(T)e^{-j2\pi fT}\mathrm{d}T = \int_{-\infty}^{-\tau_0} F_{i2}e^{-j2\pi fT}\mathrm{d}T + \\ & + \int_{-\tau_0}^{\tau_0} F_{i1}e^{-j2\pi fT}\mathrm{d}T + \int_{\tau_0}^{\infty} F_{i2}e^{-j2\pi fT}\mathrm{d}T. \end{aligned} \tag{17}$$

Combining equations (15), (16) and (17) one can write for one sided spectral power density S_i

$$\begin{aligned} S_i(f) =& (1+R)^2\delta(f) + 2Re^{-2(\tau_0/\tau_c)}\delta(f - f_b) + \\ & + \frac{2R\tau_c}{1 + \pi^2\tau_c^2(f-f_b)^2}\{1 - e^{-2(\tau_0/\tau_c)}[\cos 2\pi(f-f_b)\tau_0 \\ & + \frac{\sin 2\pi(f-f_b)\tau_0}{\pi\tau_c(f-f_b)}]\}. \end{aligned} \tag{18}$$

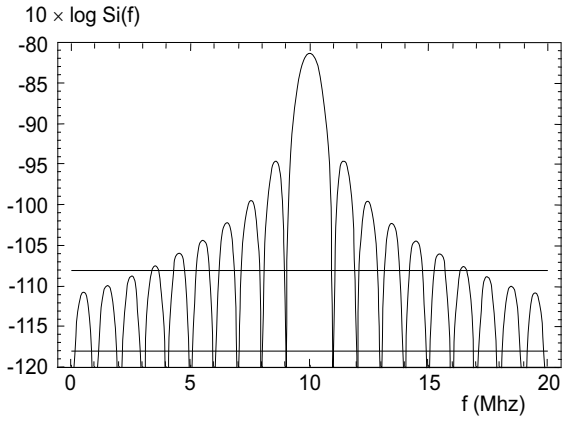

Fig. 2. Spectral power density of the phase-noise detector signal and the back-scattered signal (straight horizontal line at the level of -108 dB for the space resolution $\Delta x = 1$ cm)

The first term represents the dc component in the detector signal, the second one is the beating frequency signal due to reflection on the test fiber end. It is worth to note that this component is proportional to the reflection coefficient R and its magnitude decreases with the fiber length and with the shortening of the coherence length of the source. *This term manifests the limitation of the C-FDR as a consequence of the final coherence length of the source.* The last term corresponds to the phase noise of the source. It is drawn in Fig. 2 for the case of SM test fiber with $L = 100$m, $\tau_0 = 1\mu$s, $R = 10^{-2}$, $S = 10^{-3}$, $\alpha_s = 8 \times 10^{-5}$1/m (Rayleigh attenuation coefficient) and for the optical source spectral line-width with $\Delta\nu_0 = 10$ kHz, $\gamma = 5 \times 10^{12}$ Hz/s, $f_b = 10$ MHz. For comparison we have plotted also the power spectral density of the Rayleigh back-scattered signal in the same fiber calculated according to the formula $S_{RBS}(f) = Sv_g\alpha_s/(2\gamma)$. We can see that the phase noise is symmetrically and broadly distributed around the beating frequency component (which corresponds to the fiber end in the space domain) and can strongly dominate the back-scattered signal. *As a consequence the phase noise of the source distributed around the Fresnel reflection centers can significantly limit the sections of the fiber where the reliable measurement of the back-scattered signal is possible.*

In practical measurements one can measure the optical power of the beating frequency signal at the photodetector instead of the power density. This can be described by (18) taking $f = f_b$. The graphical plot of the last two terms, corresponding to the fiber end reflection and the phase-noise, as a function of normalized fiber length L/L_c is given in Fig. 3.

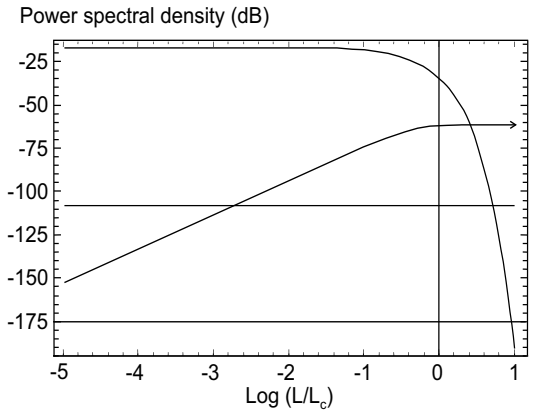

Fig. 3. Spectral power density of the reflection and phase-noise components as a function of normalized fiber length. Horizontal line at -108 dB shows the spectral power density of the Rayleigh back-scattered signal for the case of $\Delta x = 1$ cm.

The upper exponentially decreasing curve shows the decrease of the power of beating signal due to the finite source coherence length. The gradually increasing curve describes the power of the phase noise with the beating frequency. The intersection of this curve with the back-scattered power (for the space resolution 1 cm) determines the part of the fiber where the back-scattered signal can be measured at the presence of a rather strong Fresnel reflection. The knowledge of these curves make possible to "adjust" the parameters of a C-FDR based reflectometer to the required needs or to define the capabilities of a given system.

3 LIMITATIONS BY OTHER FACTORS

Other important limitations of C-OFDR are: non-linearity of the optical frequency sweep, mode hopping of the optical source, polarization effects and optical source intensity noise.

The non-linearity effect is particularly significant in semiconductor lasers. Due to a certain thermal capacity of the laser module the frequency response to the modulation current is non-linear. As a result the frequency sweep rate is not constant and the instantaneous frequency differs from that at strongly linear sweeping. The direct effect of this deviation is the broadening of the peak produced by reflection in the Fourier transform of the measured signal, what results in limiting the spatial resolution. This problem can be solved by two methods. The first utilizes an auxiliary interferometer to generate equally spaced optical frequency trigger signals for the test interferometer. The second method consists in a proper correction of modulation current so that the sweep is linear [8].

Semiconductor lasers are very sensitive to the back reflections coming from the external boundaries like FC/PC connectors creating the external cavity resonators. If the feedback from these resonators is sufficiently strong, optical frequency sweep is modulated by steps of phase. This so called "mode hopping" produces two effects in C-OFDR. One is the increase of the noise floor and the other one is the presence of spurious peaks in the output signal generated by the periodicity of the phase steps [11].

C-OFDR uses a coherent detection scheme that is very sensitive to the state of polarization of signals from both arms of the interferometer. Indeed, if the polarization of both signals is orthogonal at the detector, the coupling between the signals is erased and the reflection from the test arm cannot be recovered. Therefore strong attention must be paid to the stability of polarization during the measurement process. This problem cannot be solved here by using the polarization diversity receivers, based on separate detection of both orthogonal polarization components and subsequent summing of the detected signals, as it is the case in low coherence OTDR. C-OFDR technique uses instead of the monochromatic signal a frequency modulated one and this makes a big difference [12]. To this time there are two ways how to avoid the polarization problem. First, it is the use of the technique of polarization diversity receivers but in the frequency domain. It means that two spectrum analyzers must be used for the two orthogonal polarization components and then both spectra are to be summed. The second method consists in the use of a polarization controller in the reference arm of the reflectometer. Repeating the measurements process many times while changing the state of polarization in the reference arm in a prescribed way and subsequent averaging the measured data makes possible to remove the influence of the polarization effect [13].

5 CONCLUSION

C-OFDR is an efficient tool for the testing of optical networks and their components. Its performance parameters fulfil the gap between the traditional OTDR usually applied in testing long haul optical lines and the low coherence OTDR developed for testing short optical waveguides. C-OFDR can be efficiently used mainly for a shorter fiber length. This methods approaches very high sensitivities under (-140 dB), the space resolution less than 1 mm and dynamical range about 80 dB. The measurement range depends on the coherence length of the optical source and changes from a fraction of m to a hundred of meters. If compared with the traditional OTDR the main advantage of C-OFDR consists in the direct proportionality between the space resolution and the frequency band width of the reflectometer. It means that there is no trade-off between the dynamical range and space resolution in this method. The performance parameters of the C-OFDR are limited mainly by the finite coherence length of the optical source and by its phase noise. Serious difficulties represent also the non-linearity of the frequency sweep rate, mode hopping and polarization effects. Several solutions of these problems were published in the literature.

Acknowledgment

This work was supported by VEGA Grant 1/7603/20.

References

[1] M. K. BARNOSKI—S. M. JENSEN: Fiber waveguides, A novel Technique for Investigating of Attenuation Characteristics, Appl. Opt. **16,** (1978), 2112-2115.

[2] J. TURN—K. HNT: Fiber Optic Sensors, ALFA Publishing Co., Bratislava, 1991, pp. 225.

[3] M. ZOBOLI—P. BASSI: High Spatial Resolution OTDR Attenuation Measurements by a Correlation Technique, Appl. Opt. **22** No. 23 (1993).

[4] M. NAZARATHY—S. A. NEWTON—R. P. GIFFARD—D. S. MOBERLY—F. SISCHKA—W. R. TRUTNA—S. FOSTER: Real-Time Long Range Complementary Correlation Optical Time Domain Reflectometer, J, Lightwave Technol. **7** No. 1 (1989), 23-38.

[5] J. JASENEK—O. ČERMÁK "Photon-Counting Reflectomeyter with Correction of Measured Data", J. of Electrical Engineernig, .

[6] R. ROJKO—J. JASENEK: Low-Coherence Optical Time-Domain Reflectometry and Homogenity of Materials, J. of Electrical Engineernig **48** No. 9 (1994), 129-132.

[7] U. GLOMBITZA—E. BRINKMEYER: Coherent Frequency-Domain Reflectometry for Characterization of Single-Mode Integrated Optical waveguides, J. Lightwave Technol. **11** No. 8 (1993), 1377-1384.

[8] R. PASSY—N. GISIN—J. P. VONDERWIDE—H. H. GILDEN: Experimental and Theoretical Investigations of Coherent OFDR with Semicoductor Laser Sources, J. Lightwave Technol. **12** No. 9 (1994), 1622-1630.

[9] J. P. VONDERWIDE—R. PASSY—N. GISIN: Mid-Range Coherent Optical Frequency Domain Reflectometry with a DFB Laser Diode Coupled to External Cavity, J. Lightwave Technol. **13** No. 5 (1995), 951-960.

[10] P. OBERSON—B. HUTTNER—O. GUINNARD—L. GUINNARD—G. RIBORDY—N. GISIN: Optical Frequency Domain Reflectometry with a Narrow Linewidth Fiber Laser, IEE Photon. Tech. Letters **12** No. 7 (2000), 867-869.

[11] R. PASSY—N. GISIN—J. P. VONDERWIDE: Mode hopping in coherent FMCW refelectometry, Electron. Lett. **28** No. 23 (1992), 2186.

[12] W. V. SORIN—L. HEFFNER: Polarization independent interferometric coherence-domain reflectometry", US Patent 95 202 745, 1993.

[13] G. MUSSI—P. STAMP—N. GISSIN—R. PASSY—J. P. VONDERWIDE: Polarization Effects in Coherent Optical Frequency-Domain Reflectometry, IEEE Photon. Tech. Lett. **11** No. November (1996), 1513-1515.

Received 25 May 2001

Jozef Jasenek (Doc, Ing, PhD), born in 1947, Bobrov (Northern Slovakia), graduated from the Faculty of Electrical Engineering and Information Technology of the Slovak University of Technology Bratislava in 1971, in solid state physics. PhD studies completed in 1980. Appopinted Associate Professor for Electromagnetic field theory in 1986. After graduation he joined the Faculty of Electrical Engineering and Information Technology of the Slovak University of Technology Bratislava, Department of Electromagnetic Theory and has been working there to this time. During the years 1994 - 2000 he served as a vice-dean responsible for the pedagogical affairs. His former professional interests concern the development and application of microwave ferrite materials for microwave circuit components design. Now he is engaged in the theory of linear and nonlinear optical waveguides and in the development of experimental methods for the testing of optical waveguides and optical fiber two-port components. Especially he is interested in the analysis and implementation of optical reflectometric methods (OTDR an its modifications). He was awarded by several scientific grants and has published more than 40 scientific papers in journals or presented in scientific conferences at home and abroad.